



Transactions, SMiRT-26
Berlin/Potsdam, Germany, July 10-15, 2022
Division V

A FRAMEWORK FOR CHARACTERIZING CYCLIC BEHAVIOR OF PIPING T-JOINT CONNECTIONS HAVING DIFFERENT BOUNDARY CONDITIONS

Mrinal Jyoti Mahanta¹, Abhinav Gupta², Sung Gook Cho³, Gihwan So⁴

¹ Doctoral Student, North Carolina State University, USA (mjmahant@ncsu.edu)

² Director, Center for Nuclear Energy Facilities and Structures (CNEFS), North Carolina State University

³ CEO, R&D Center, Innose Tech Co., LTD, Incheon, Republic of Korea

⁴ Researcher, R&D Center, Innose Tech Co., LTD, Incheon, Republic of Korea

ABSTRACT

The 1971 San Fernando and the 1994 North Ridge earthquakes highlighted that one of the primary reasons for damage in critical facilities like hospitals is the water leakage observed at the T-joint connections of piping systems. Therefore, a proper understanding of the functioning of T-joint having different boundary conditions under the effect of cyclic loading is essential to characterize the failure of the T-joints. This paper presents the experimental results of a study on T-joint connections with different boundary conditions and reconciliation of the experimental results with the corresponding simulation results. In the experiments, constant loading amplitudes for a prescribed number of cycles are applied on the T-joint. For the hinge boundary condition, the loading amplitudes considered in the experiments are 15 mm, 17 mm, 18 mm, 19 mm, and 20 mm respectively. Similarly, the loading amplitude considered for the fixed boundary conditions are 5 mm, 9 mm, 11 mm, 15 mm, and 19 mm respectively. It is found out that the simulation results reconcile well with the experimental results when “pinching” model is used to represent the nonlinear moment-rotation behaviour of a T-joint in the piping system.

INTRODUCTION

Observations from past earthquake-related failures of piping systems in non-nuclear facilities such as hospitals and industrial plants have highlighted that such failures take place primarily at the location of T-joints. Such failures also lead to a shutdown of either a part of the facility or the entire facility, which impacts the recovery of a region following a major disaster. For example, in the 1994 Northridge earthquake, the Olive View hospital suffered significant damages from internal flooding caused by the piping failure at the T-joint location (Ayers, 1996; Ayers and Philips, 1998; Reitherman and Sabol, 1995). As a result, the hospital had to be shut down for a prolonged period. Therefore, to comprehend the behavior of the T-joint under the effect of cyclic loading, many recent studies (Ju and Gupta, 2015; Ryu et al., 2016) emphasized the importance of performing experiments on the T-joint component of a piping system. This paper presents the results of a detailed experimental study on the T-Joint and addresses several vital aspects in the fragility assessment of T-joints in a piping system. More specifically, it presents the results on the following two aspects:

- Behavior of the T-joint with different boundary conditions under the effect of the constant amplitude cyclic loading.
- Reconciliation of the experimental result on the T-joint for the different boundary conditions with the corresponding results from nonlinear analyses.

EXPERIMENTAL TEST SET-UP

As the type of boundary conditions affects the dynamic behavior of a T-joint component, laboratory tests are performed on T-joint piping components with two types of boundary conditions: hinge and fixed. For the experiments, carbon pipes (KS D 3507 SPP) with a thickness of 3.3 mm and an outside diameter of 34 mm are used. Figures 1 and 2 show the experimental setup used in the laboratory for the T-joint component with hinge and fixed boundary conditions, respectively.

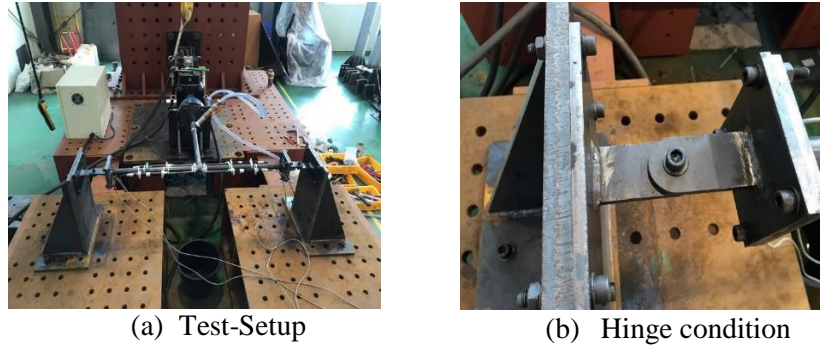


Figure 1. Test setup of T-joint component having hinge boundary condition

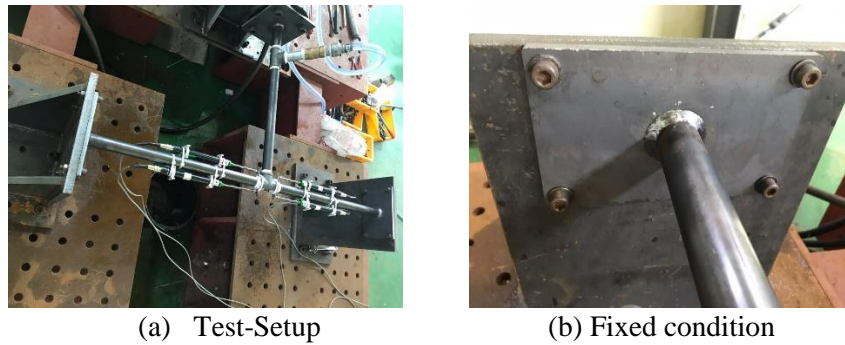


Figure 2. Test-set up of T-joint component having fixed boundary condition

During the experiments, an in-plane loading of constant amplitudes are applied for ten cycles at the bottom of the T-joint component for both fixed and hinge boundary conditions. For the hinge boundary conditions, the loading amplitudes considered in the experiment are 15 mm, 17 mm, 18 mm, 19 mm, and 20 mm, respectively. On the other hand, the loading amplitudes considered for the fixed boundary conditions are 5 mm, 9 mm, 11 mm, 15 mm, and 19 mm respectively. For illustration, the cyclic loading amplitude of 15 mm is shown in Figure 3.

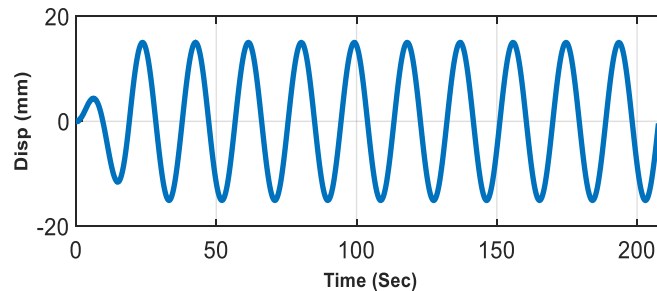
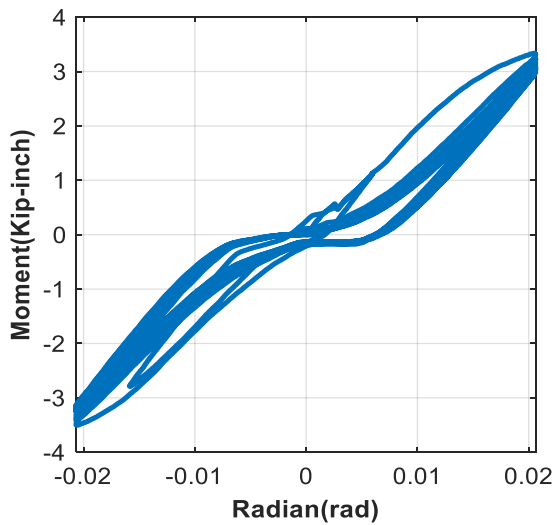


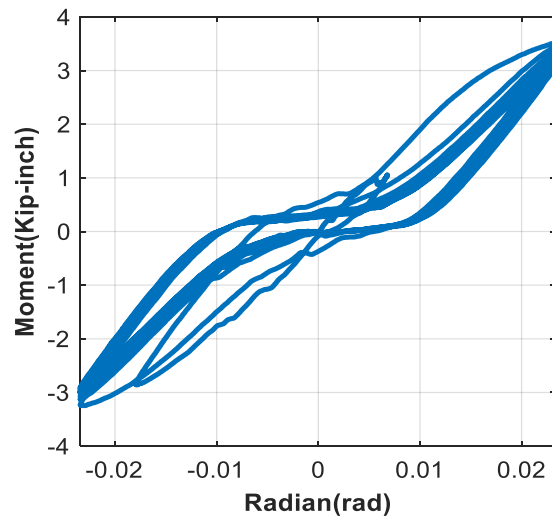
Figure 3. Cyclic loading of 15 mm amplitude

EXPERIMENTAL RESULT

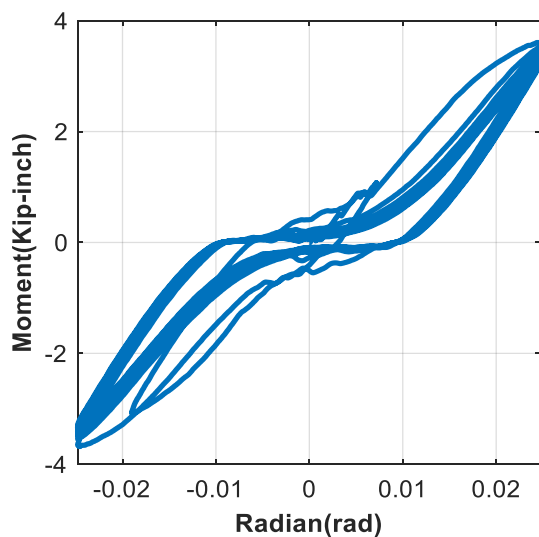
For both the hinge and the fixed boundary conditions of the T-joint component, experimental results for the moment-rotation curves recorded at the T-joint location are plotted for each applied loading protocol of constant amplitude. It has been observed that the number of loading cycles required to cause the leakage at the T-Joint connection is governed by displacement loading amplitude applied on the T-Joint connection. As the loading amplitude increases, the number of loading cycles required to cause the leakage at the T-Joint connection decreases. However, for the 15 mm loading amplitude, no leakage is observed at the T-Joint connection because the total numbers of loading cycles used are likely less than the number of cycles needed for low-cycle fatigue failure. Figure 4 shows the experimental results of the moment rotation response at the T-joint connection for the hinge boundary condition. In these figures shown below, the moment-rotation responses at the T-joint connection are plotted till the first leakage of the T-joint.



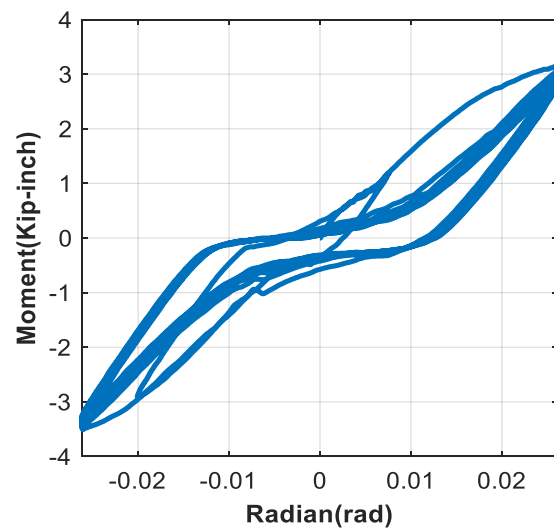
(a) 15 mm loading amplitude



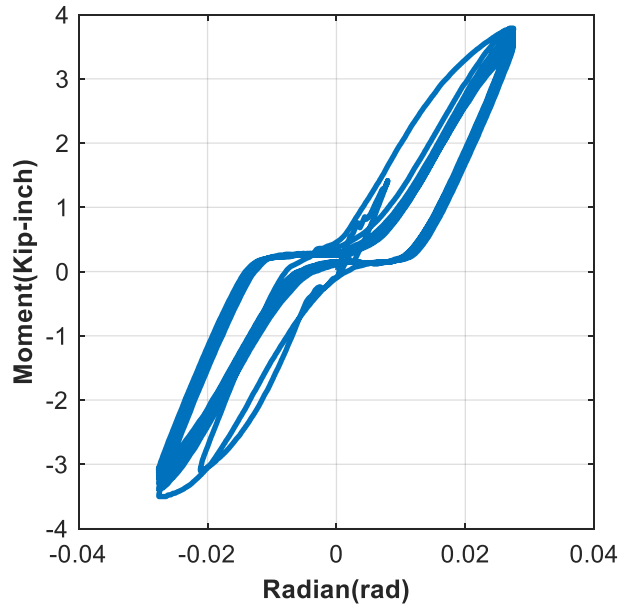
(b) 17 mm loading amplitude



(c) 18 mm loading amplitude



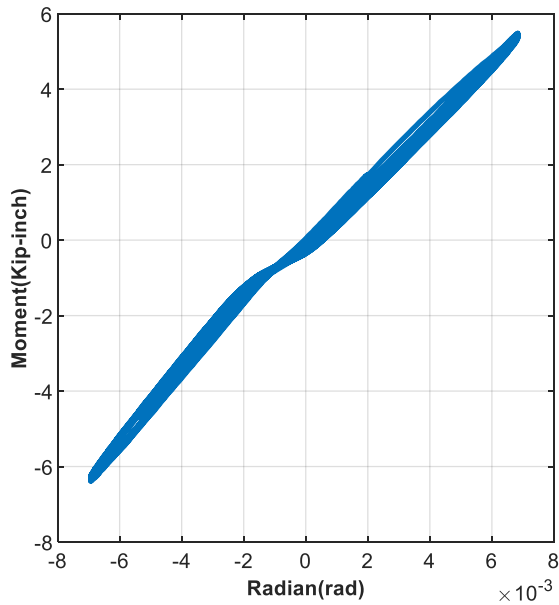
(d) 19 mm loading amplitude



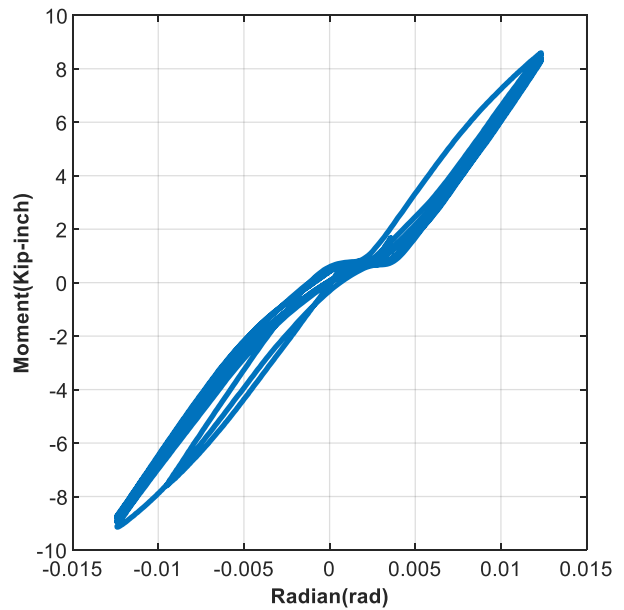
(d) 20 mm loading amplitude

Figure 4. Experimental result for the hinge boundary condition

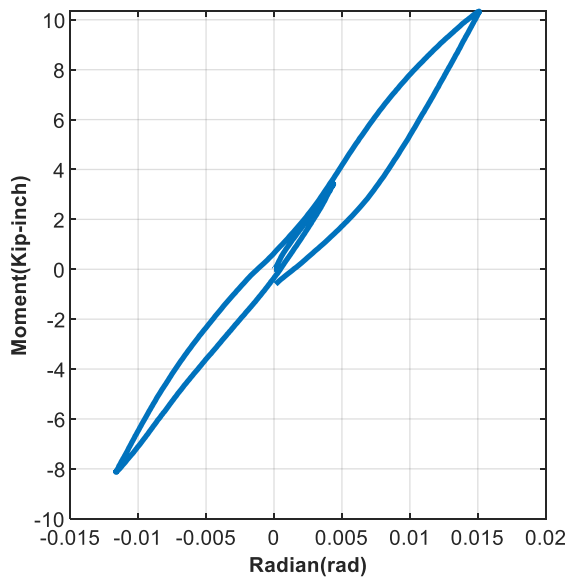
Similarly, Figure 5 shows the experimental results of moment rotation at the T-joint for the fixed boundary condition till the first leakage of the T-joint.



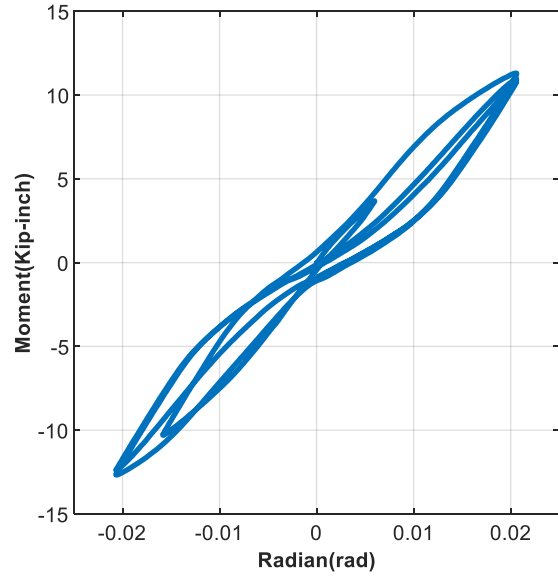
(a) 5 mm loading amplitude



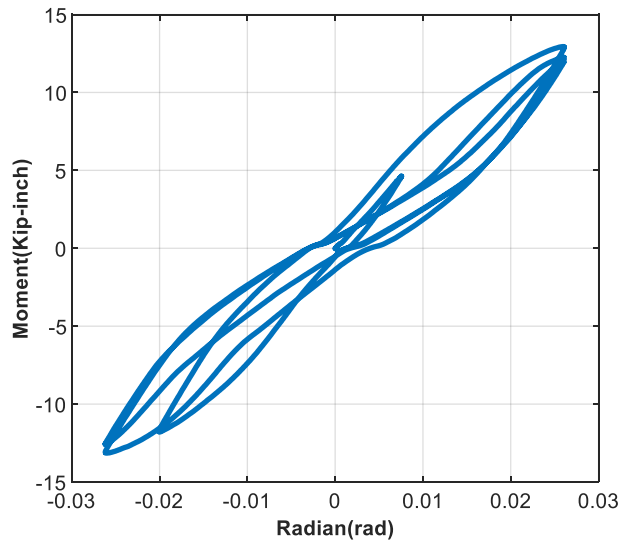
(b) 9 mm loading amplitude



(c) 11 mm loading amplitude



(d) 15 mm loading amplitude



(e) 19 mm loading amplitude

Figure 5. Experimental result for the Fixed boundary condition

COMPUTATIONAL MODELING OF T-JOINT COMPONENT

For the reconciliation of the experimental result with the simulation result, Opensees (Mazzoni et al., 2006) software is used for the numerical modeling of the T-joint component. The T-joint connections and the branch on either side of the connection are modeled using nonlinear rotational springs and frame elements, respectively. Finally, the cyclic loads are applied as in-plane axial load along the web at the bottom of the T-joint component, as shown in figure 6(a).

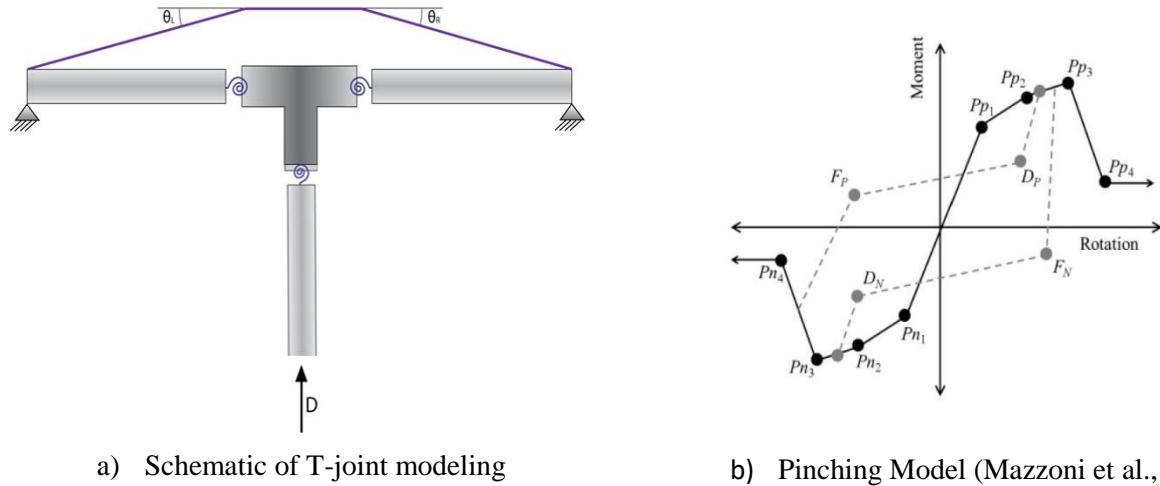
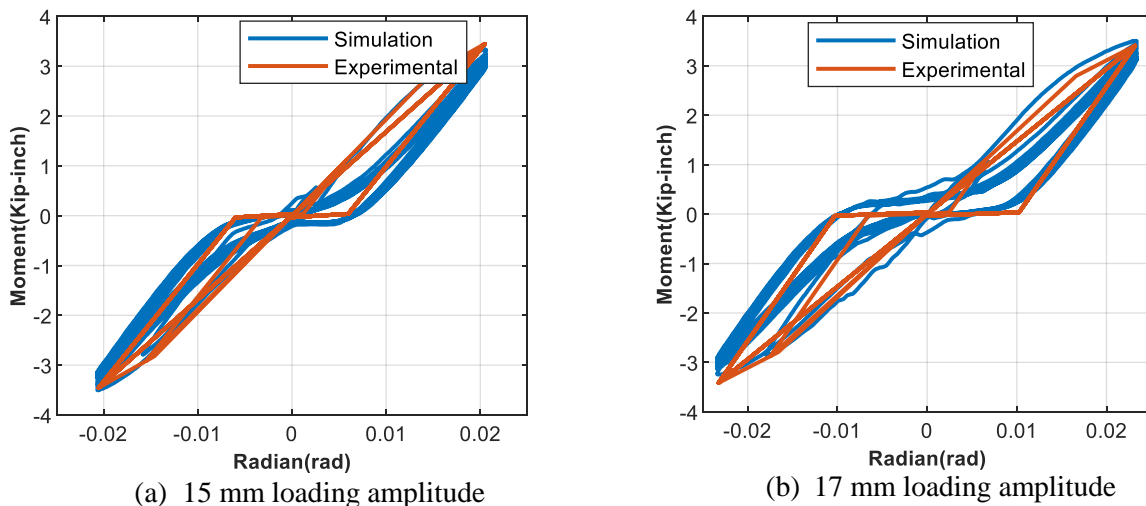


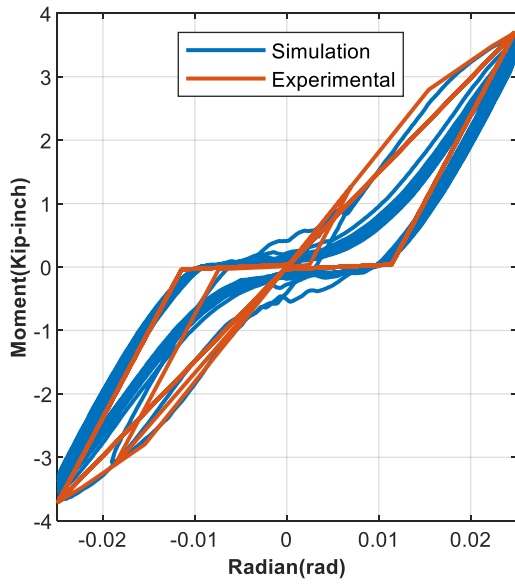
Figure 6. Schematic of the T-joint modeling

The “Pinching” model available in the Opensees (Mazzoni et al., 2006) is used to model the nonlinear springs for characterization of the hysteresis response of the T-joint connection under cyclic loadings. Figure 6(b) shows the schematic of the “pinching” model used in this study. To characterize the hysteresis responses of the “Pinching Model”, a total of eight points are required to be defined. Four of these points, P_{p1} , P_{p2} , P_{p3} and P_{p4} correspond to the moments under the positive loading direction, and the remaining four points, P_{n1} , P_{n2} , P_{n3} and P_{n4} correspond to the moments under the negative loading direction. F_p and F_n define the strength ratio for unloading from a negative and a positive load, respectively. In addition, D_n and D_p represent the points at which the reloading starts.

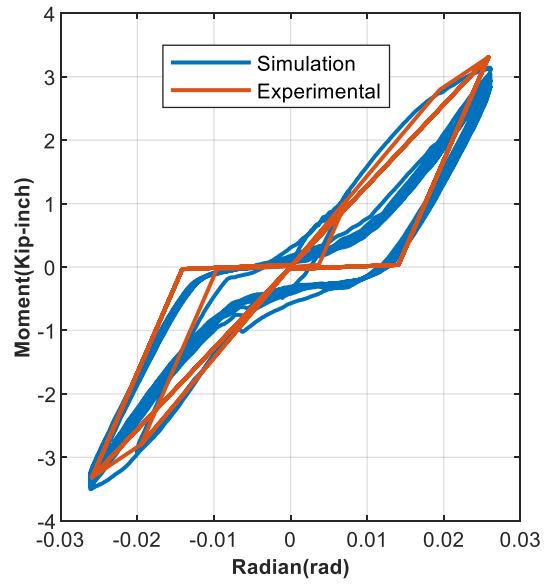
RECONCILIATION OF THE EXPERIMENTAL RESULT WITH THE SIMULATION RESULT

Figure 7 shows the reconciliation of the experimental results of the moment rotation curve for the T-joint connection with the simulation results in case of the hinge boundary condition.

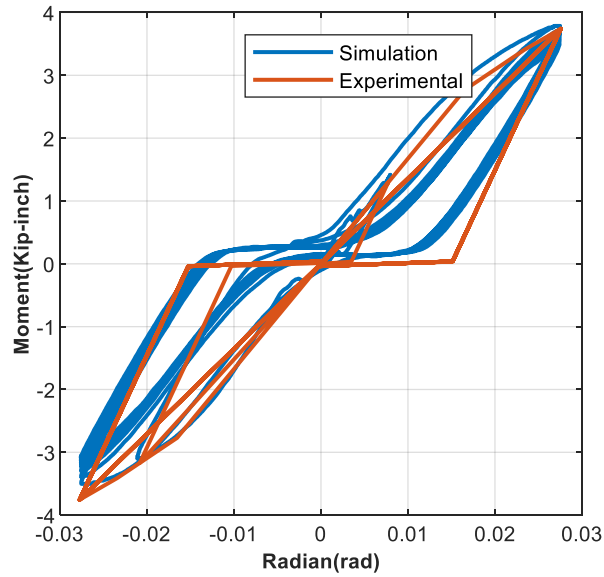




(c) 18 mm loading amplitude



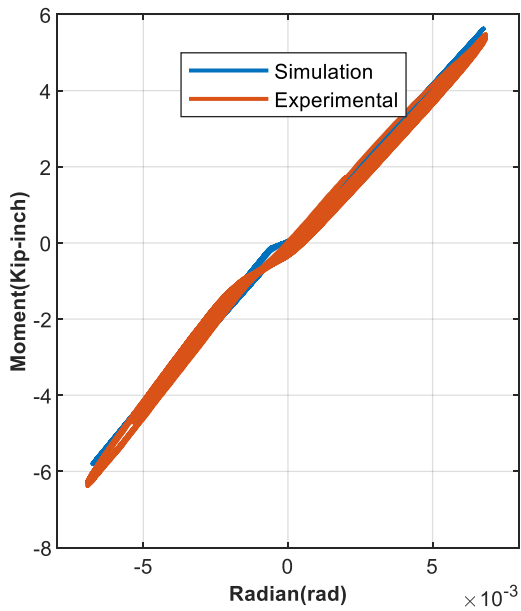
(d) 19 mm loading amplitude



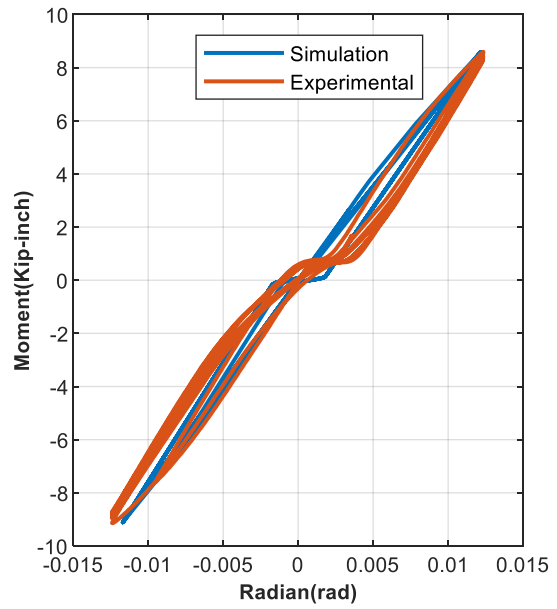
(e) 20 mm loading amplitude

Figure 7. Comparison of experimental result with simulation

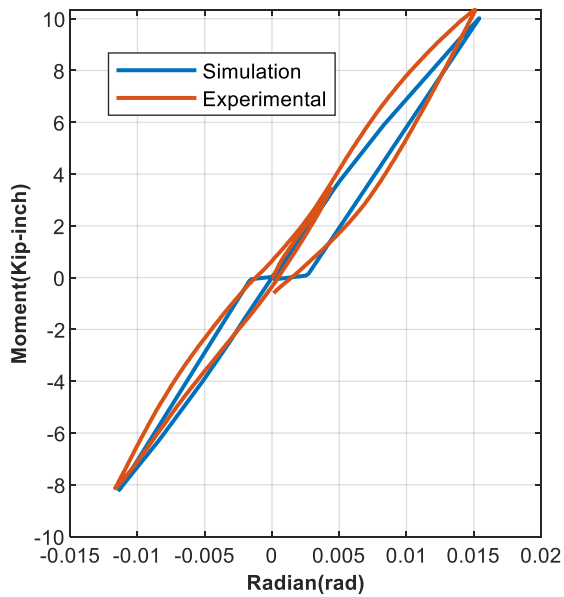
Similarly, the reconciliation of the experimental results of the moment rotation of the T-joint connection with the simulation results in the case of fixed boundary conditions is shown in Figure 8.



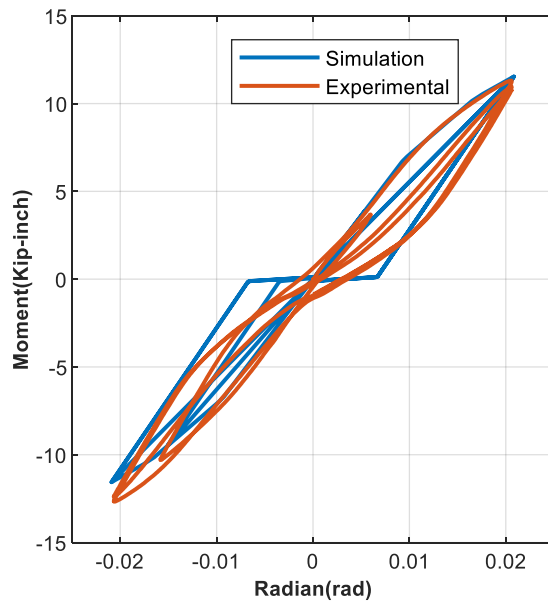
(a) 5 mm loading amplitude



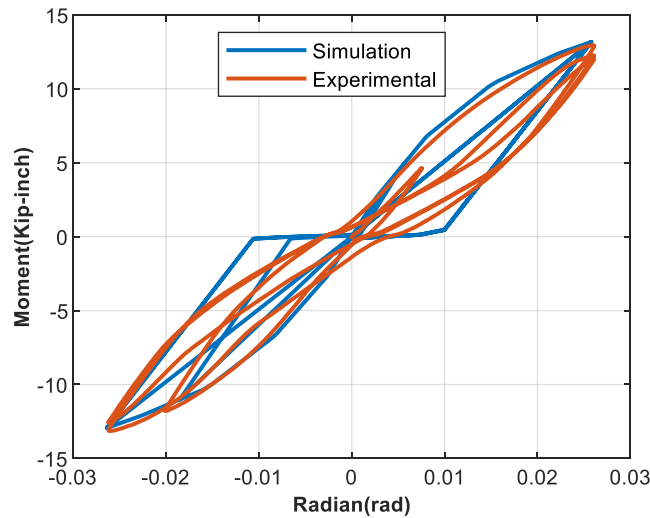
(b) 9 mm loading amplitude



(c) 11 mm loading amplitude



(d) 15 mm loading amplitude



(e) 19 mm loading amplitude

Figure 8. Comparison of the experimental results with simulation

From the reconciliation of the moment-rotation plot of T-joint for the hinge and the fixed boundary conditions under the effect of cyclic loading, it is evident that the boundary condition of the T-joint affects the strength and the effective stiffness of the moment-rotation plot. The effective stiffness is defined as a ratio of maximum moment to the maximum rotation as shown in Equation 1.

$$\text{Effective Stiffness} = \frac{\text{Maximum Moment}}{\text{Maximum Rotation}} \quad (1)$$

Tables 1 and 2 show the differences in the strength and effective stiffness for the moment rotation plot of the T-joint under the cyclic load with an amplitude of 15 mm and 19 mm, respectively.

Table 1: Comparison for the 15 mm loading amplitude

Measured quantity	Hinge Boundary	Fixed Boundary
Strength (kip-inch)	3.21	11.29
Effective Stiffness (Kip-inch)	156.31	548.48

Table 2: Comparison for the 19 mm loading amplitude

Measured quantity	Hinge Boundary	Fixed Boundary
Strength (kip-inch)	3.42	12.95
Effective Stiffness (Kip-inch)	131.01	495.68

CONCLUSIONS

The key conclusions of this study are summarized as follows:

- The moment-rotation responses at the T-joint connection from the simulation and the experiments agree well.
- The “pinching” model available in the Opensees can serve well for modeling the T-joint hysteretic behavior.
- No leakage is observed for the 15 mm loading amplitude for hinge boundary conditions. For all other loading amplitude, as the loading amplitude increases, the number of loading cycles till the first leakage decreases.
- For a given loading amplitude, it has been observed that the maximum moment and the effective stiffness of the moment-rotation plot are higher for the fixed boundary condition than for the hinge boundary condition.

REFERENCES

- Ayers, J. Marx. (1996). “*Northridge Earthquake Hospital Water Damage Study*”, Ayers & Ezers Associates, Inc. Los Angeles, California.
- Ayres, J. M. and Phillips, R. J. (1998). “*Water Damage in Hospitals Resulting from the Northridge Earthquake,*” ASHRAE Trans., American Society of Heating, Refrigerating and Air-Conditioning Engineers, Atlanta, Georgia, Vol. 104, Part 1.
- Ju, Bu Seog., Gupta, A. (2015). “*Seismic fragility of threaded Tee-joint connections in piping systems*”, International Journal of Pressure Vessels and Piping, Volume 132-133 pages 106-118.
- Mazzoni, S., McKenna, F., Scott, M. H. and Fenves, G. L. (2006). “*OpenSees Command Language Manual,*” Open System for Earthquake Engineering Simulation (OpenSees), <http://opensees.berkeley.edu/>
- Reitherman, R., and Sabol, T. A. (1995). “*Northridge Earthquake of January 17, 1994: Reconnaissance Report—Nonstructural Damage,*” Earthquake Spectra, Volume 11(S2), pp. 453– 514.
- Ryu, Y., Gupta, A., Woo Y. J. and Ju, Bu Seog. (2016). “*A Reconciliation of Experimental and Analytical Results for Piping Systems*”, International Journal of Steel Structures, Volume 16, Issue 4, pages 1043–1055.